arXiv:cond-mat/0402228v1 [cond-mat.mes-hall] 8 Feb 2004

Low frequency current noise of the single-electron shuttle

A. Isacsson[1,2]*and T. Nord[2]

[1]*Department of Physics, Yale University, P.O. Box 208120, New Haven CT 06520-8120*
[2] *Department of Applied Physics, Chalmers University of Technology and Göteborg University, SE-412 96 Göteborg, Sweden*

Abstract

Coupling between electronic and mechanical degrees of freedom in a single electron shuttle system can cause a mechanical instability leading to shuttle transport of electrons between external leads. We predict that the resulting low frequency current noise can be enhanced due to amplitude fluctuations of the shuttle oscillations. Moreover, at the onset of mechanical instability a pronounced peak in the low frequency noise is expected.

*Email:isac@fy.chalmers.se

1 Introduction

Charge transport in nanostructures is a major research area, both theoretically and experimentally. Apart from the average current flowing through a structure in response to an applied external field, fluctuations and correlations in time of this current are of interest. By studying the current noise power spectral density (PSD), information about the charge transport process can be extracted that may not be accessible through studies of the average current alone.[1] An example of this is shot noise, arising due to the discreteness of the charge carriers, (electrons). [2]

In Nanoelectromechanical Systems (NEMS) [3], mechanical degrees of freedom affect and/or are affected by charge transport through the device. One such system is the single electron shuttle system [4], also known as the nanoelectromechanical single electron transistor (NEM-SET). The system consists of a metallic grain embedded in an elastic material between two bulk leads, forming a mechanically soft Coulomb blockade double junction. Since current through the system is accompanied by charging of the grain, interplay between the Coulomb forces and the mechanical degrees of freedom can lead to self-oscillations of the grain, which in turn, supports charge transport through shuttling of electrons between the leads. Much work, both experimental [5, 6, 7, 8, 9] as well as theoretical [4, 10, 11, 12, 13, 14, 15, 16, 17, 18, 19, 20, 21, 22, 23, 24] has been reported in this field.

In this paper, the noise spectrum of the single-electron shuttle is studied in the limit of weak electromechanical coupling. It is found that the onset of mechanical vibrations is accompanied by a peak in the low frequency PSD. Hence, by measuring the noise, it can be determined whether or not the grain is oscillating. This is an important result since direct detection of any high frequency mechanical motion is problematic with present day experimental techniques.

2 Model System

A schematic picture of the system is shown in fig. 1a. A metallic grain of mass M and radius r is placed between two leads, separated by a distance L, via elastic, insulating materials. When a bias voltage $V \equiv (V_L - V_R)$ is applied between the leads, electron transport occur by sequential, incoherent, tunneling between the leads and the grain. The system can also lower its electrostatic energy by altering the grain position X.

The electron transport in the system is described using the notion of the equivalent circuit of fig. 1b characterized by resistances and capacitances $R_{L,R}$ and $C_{L,R}$ which both depend on the grain position X:

$$R_{L,R}(X) = R_0^{L,R} \exp(\pm X/\lambda),\ C_{L,R}(X) = C_0^{L,R}/(1 \pm X/A_{L,R}).$$

Here λ is the characteristic length scale for tunneling and $C_0^{L,R}$ are the capacitances of the left and right junctions when the grain is at $X = 0$. The coefficients

$A_{L,R}$ are typical capacitance length scales for the left and right tunnel junction respectively. The grain self-capacitance C_0 is also included in the model.

If $E_C \gg \hbar/R(X)C(X)$, where $E_C = e^2/2C$, tunneling is well described by the "orthodox" theory of Coulomb blockade [25] and the tunneling rates through the left(right) junction is

$$\Gamma^{\pm}_{L,R}(X,V,Q) = \frac{\Delta G^{\pm}_{L,R}(X,V,Q)}{e^2 R_{L,R}(X)} \frac{1}{1-e^{-\beta \Delta G^{\pm}_{L,R}(X,V,Q)}}. \quad (1)$$

Here β is the inverse temperature and $\Delta G^{\pm}_{L,R}(X,V,Q)$ is the decrease of free energy as the event $(Q, Q_{L,R}) \rightarrow (Q \pm e, Q_{L,R} \mp e)$ occurs. The charges $Q_{L,R}$ and Q denote the charges accumulated on the left and right leads and the excess charge on the grain. The free energy decrease $\Delta G^{\pm}_{L,R}(X,V,Q)$ can be expressed using the equivalent circuit model of fig. 1b.

Considering the grain motion to be classical and one dimensional we have Newton's equation $M\ddot{X} = F_{\text{Ext.}}(X,V,Q)$ for the grain displacement. The external force $F_{\text{Ext.}}(X,V,Q)$ acting on the grain includes an elastic force $F_k(X)$, a dissipative force $F_\gamma(\dot{X})$, an electric force $F_\epsilon(X,Q,V)$ and a vdW force $F_{vdW}(X)$ yielding the equation of motion

$$M\ddot{X} = F_k(X) + F_\gamma(\dot{X}) + F_\epsilon(X,Q,V) + F_{vdW}(X). \quad (2)$$

For the elastic force we use a phenomenological non-linear potential [13] acting as a harmonic well with spring force constant k for small displacements but that diverges as a Lennard-Jones potential (12th power) at the positions X_L and X_R:

$$F_k(X) = \frac{a}{(X+X_L)^{13}} + \frac{b}{(X-X_R)^{13}},$$

where

$$a = -\frac{k}{13}\frac{(X_0-X_R)(X_0+X_L)^{14}}{X_L+X_R},\ b = \frac{k}{13}\frac{(X_0+X_L)(X_0-X_R)^{14}}{X_L+X_R}.$$

The dissipative force is modelled as a viscous damping term $F_\gamma(\dot{X}) = -\gamma\dot{X}$, and the electrostatic force is given by

$$F_\epsilon(X,V,Q) = \frac{1}{2}\frac{dQ_L}{dX}V_L + \frac{1}{2}\frac{dQ_R}{dX}V_R - \frac{1}{2}Q\frac{dV}{dX},$$

where Q and $V_{L,R}$ can be calculated from the equivalent circuit of fig. 1b. Finally, the van der Waals force between the grain and the leads is derived from a Lennard-Jones interaction potential for the individual atoms [26] in the leads and the grain respectively. For a geometry with a metallic sphere close to a flat substrate one finds,

$$\begin{aligned} F_{vdW} &= \frac{H_a}{6}\left(\frac{r}{\left(\frac{L}{2}-r-X\right)^2} - \frac{r}{\left(\frac{L}{2}-r+X\right)^2}\right) \\ &- \frac{H_r}{180}\left(\frac{r}{\left(\frac{L}{2}-r-X\right)^8} - \frac{r}{\left(\frac{L}{2}-r+X\right)^8}\right), \end{aligned}$$

where $H_{a,r}$ are the Hamaker constants for the attractive and repulsive parts of the force. Equation (2) together with eq. (1) describe the dynamics of the system.

3 Features of the noise spectrum

In this section we will briefly describe the current noise-spectrum of the model system presented in the previous section. Defining the current I through the system as the charge transferred per unit time from the grain to the right lead, the PSD is given by

$$S_{II}(\omega) \equiv 2 \int_{-\infty}^{+\infty} dt e^{i\omega t} \langle \Delta I(t) \Delta I(0) \rangle$$

where the brackets denotes ensemble averaging. [27] By doing direct numerical integration, *i.e.* solving the stochastic differential equation eq. (2), the current as a function of time is obtained and the noise spectrum calculated. A representative result of such a calculation is shown in fig. 2. This spectrum was calculated for a system in the shuttle regime. The PSD has been normalized to obtain the Fano factor $F = S_{II}/(2e \langle I \rangle)$.

We have divided the spectrum in fig. 2 into four regions marked **I-IV**. At high frequencies, region **IV**, the Fano factor is close to a value of 1/2 which is the value for a static double junction [27]. In region **III** two strong peaks are located at the vibration frequency and the first harmonic. This is a result of the periodic charging and decharging of the oscillating grain. The large magnitude of the first harmonic stems from the fact that charge exchange between the grain and the left lead gives rise to a displacement current in the right lead where we measure I. Directly below the peaks, region **II**, the noise is suppressed below the shot noise level of a static double junction, possibly due to the additional in time correlations between successive tunnel events induced by the oscillating grain.

The most interesting part of the spectrum however, is the low frequency part in region **I**, where the Fano factor increases. This enhancement of the noise is associated with fluctuations in mechanical energy. In the next section we present an analytical treatment of a simplified model system which does not take into account non-linear elastic forces, vdW forces or position dependent capacitances. Nevertheless, this model suffices to explain the low frequency behavior of the noise spectrum in the shuttle regime as well as to predict a (quasi) singular behavior of the Fano factor at the instability threshold.

4 Low frequency noise for weak electromechanical coupling

The system is completely described by the conditional probability densities $p(X, \dot{X}, Q, t | X_0, \dot{X}_0, Q_0, t_0)$ to find the system with charge Q at time t in the

interval $[X, X+dX), [\dot{X}, \dot{X}+d\dot{X})$ given it was located around $(X_0, \dot{X}_0, Q_0)$ at time t_0. The time evolution of the conditional probability density, as well as the unconditional probability density $p(X, \dot{X}, Q, t)$, is given by the phase space equation

$$\begin{aligned}
\frac{\partial}{\partial t}p(X,\dot{X},Q,t) &= -\frac{\partial}{\partial X}\left(\dot{X}p(X,\dot{X},Q,t)\right) \\
&+ \frac{\partial}{\partial \dot{X}}\left(\frac{\gamma\dot{X}-kX+F(Q)}{M}p(X,\dot{X},Q,t)\right) \\
&+ \sum_{Q'\neq Q}\Gamma_{Q'\to Q}(X)p(X,\dot{X},Q',t) \\
&- \sum_{Q'\neq Q}\Gamma_{Q\to Q'}(X)p(X,\dot{X},Q,t). \qquad (3)
\end{aligned}$$

Here a simplified version of the external force $F_{\rm Ext.} = \gamma\dot{X} - kX + F(Q)$ where $F(Q) \equiv F_\epsilon(X=0,Q,V)$ has been used. Introducing action-angle variables (E,ϕ) defined through $(X,\dot{X}) = \sqrt{2E/M\omega^2}\left(\sin(\phi), \omega\cos(\phi)\right)$, where $\omega^2 \equiv k/M$, eq. (3) takes the form

$$\begin{aligned}
\frac{\partial}{\partial t}p(E,\phi,Q,t) &= -\frac{\partial}{\partial \phi}\left(\left[\omega + \frac{\gamma}{M}\sin\phi\cos\phi - \frac{F(Q)\sin\phi}{\sqrt{2ME}}\right]p(E,\phi,Q,t)\right) \\
&- \frac{\partial}{\partial E}\left(\left[-2\frac{\gamma}{M}E\cos^2\phi + \sqrt{\frac{2E}{M}}F(Q)\cos(\phi)\right]p(E,\phi,Q,t)\right) \\
&+ \sum_{Q'\neq Q}\Gamma_{Q'\to Q}(E,\phi)p(E,\phi,Q',t) \\
&- \sum_{Q'\neq Q}\Gamma_{Q\to Q'}(E,\phi)p(E,\phi,Q,t). \qquad (4)
\end{aligned}$$

To facilitate an analytical treatment it is convenient to rewrite eq. (4). We thus introduce the dimensionless quantities $\tau = t\omega$, $n = Q/e$, $f_n = F(ne)/F(e)$, $\mathcal{E} = E/(\frac{1}{2}M\omega^2\lambda^2)$, $\tilde{\Gamma}_{n\to n'} = \omega^{-1}\Gamma_{n\to n'}$, $\epsilon = F(e)/k\lambda$, and $\eta = \gamma/(M\omega\epsilon)$. The probability density can be written in vectorial form as $\mathbf{P}(\mathcal{E},\phi,\tau)$, where the $i-th$ component is given by $p(\mathcal{E},\phi,n(i),\tau)$ with $n(i) \equiv (-1)^{i-1}\mathrm{Int}\left[\frac{i}{2}\right]$. We also introduce the matrices

$$\hat{I}_{i,j} = \delta_{i,j},\ \hat{f}_{i,j} \equiv \delta_{i,j}f_{n(i)},\ \hat{\Gamma}^+_{i,j} = \tilde{\Gamma}_{n(j)\to n(i)},\ \hat{\Gamma}^-_{i,j} = \delta_{i,j}\sum_{n'}\tilde{\Gamma}_{n(i)\to n'},$$

and, define three operators $\hat{\mathcal{L}}_1 = -\frac{\partial}{\partial\phi} + \hat{\Gamma}^+(\mathcal{E},\phi) - \hat{\Gamma}^-(\mathcal{E},\phi)$,
$\hat{\mathcal{L}}_2 = \frac{\partial}{\partial\phi}\left[\frac{\hat{f}}{\sqrt{\mathcal{E}}}\sin\phi - \hat{I}\eta\sin\phi\cos\phi\right]$, and $\hat{\mathcal{L}}_3 = 2\frac{\partial}{\partial\mathcal{E}}\left[\hat{I}\eta\mathcal{E}\cos^2\phi - \hat{f}\sqrt{\mathcal{E}}\cos\phi\right]$.
Equation (4) can then be compactly written as

$$\frac{\partial}{\partial\tau}\mathbf{P}(\mathcal{E},\phi,\tau) = \left[\hat{\mathcal{L}}_1 + \epsilon\left(\hat{\mathcal{L}}_2 + \hat{\mathcal{L}}_3\right)\right]\mathbf{P}(\mathcal{E},\phi,\tau).$$

Since the low frequency noise is governed by a time scale much longer than the period of vibration, adiabatic elimination of fast variables can be used to treat slow fluctuations in amplitude. This amounts to doing perturbation theory in ϵ.

Following ref. [28] we let $\mathbf{P}_\lambda$ and $\mathbf{Q}_\lambda$ be normalized eigensolutions to $\hat{\mathcal{L}}_1\mathbf{P}_\lambda = \lambda(\mathcal{E})\mathbf{P}_\lambda$ and $\hat{\mathcal{L}}_1^\dagger\mathbf{Q}_\lambda = \lambda^*(\mathcal{E})\mathbf{Q}_\lambda$, corresponding to eigenvalue λ. $\mathbf{P}_0(\mathcal{E},\phi)$ is the stationary solution to the unperturbed problem, i.e., $\hat{\mathcal{L}}_1\mathbf{P}_0 = 0$, while $\mathbf{Q}_0$ solves the adjoint equation $\hat{\mathcal{L}}_1^\dagger\mathbf{Q}_0 = 0$. The projector $\hat{\mathcal{P}}_0$ onto this state acting on an arbitrary vector $\mathbf{x}(\mathcal{E},\phi,\tau)$ is given by

$$\left(\hat{\mathcal{P}}_0\mathbf{x}\right)(\mathcal{E},\phi,\tau) = \mathbf{P}_0(\mathcal{E},\phi)\int_0^{2\pi} d\phi'\mathbf{Q}_0^*(\mathcal{E},\phi')\cdot\mathbf{x}(\mathcal{E},\phi',\tau).$$

By direct insertion, using that $\hat{\mathcal{L}}_1^\dagger = \frac{\partial}{\partial\phi} + \hat{\mathcal{G}}^\top(\mathcal{E},\phi)$, one finds that $(\mathbf{Q}_0)_n = [1,1,\cdots,1]^\top$. Next, splitting up $\mathbf{P}(\mathcal{E},\phi,\tau)$ in mutually orthogonal parts $\mathbf{v} \equiv \hat{\mathcal{P}}_0\mathbf{P}$ and $\mathbf{w} \equiv (1-\hat{\mathcal{P}}_0)\mathbf{P}$, an equation, correct to second order in ϵ, can be found for $\mathbf{v}$;

$$\frac{\partial}{\partial\tau}\mathbf{v} = \epsilon\hat{\mathcal{P}}_0\hat{\mathcal{L}}_4\mathbf{v} - \epsilon^2\hat{\mathcal{P}}_0\hat{\mathcal{L}}_3\hat{\mathcal{L}}_1^{-1}[\hat{\mathcal{L}}_2 + \hat{\mathcal{L}}_3 - \hat{\mathcal{P}}_0\hat{\mathcal{L}}_4]\mathbf{v}. \tag{5}$$

Here $\epsilon\hat{\mathcal{L}}_4 = \hat{I}\frac{\partial}{\partial\mathcal{E}}[\gamma(\mathcal{E}) - \mathcal{W}(\mathcal{E})]$, which contains the average dissipation per cycle $\gamma(\mathcal{E})$ and the average pumped energy per cycle $\mathcal{W}(\mathcal{E})$ defined through

$$\gamma(\mathcal{E}) \equiv 2\epsilon\eta\mathcal{E}\int_0^{2\pi} d\phi\mathbf{Q}_0^*\cdot\mathbf{P}_0(\mathcal{E},\phi)\cos^2\phi,\ \mathcal{W}(\mathcal{E}) = 2\epsilon\sqrt{\mathcal{E}}\int_0^{2\pi} d\phi\mathbf{Q}_0^*\cdot\hat{f}\mathbf{P}_0(\mathcal{E},\phi)\cos\phi.$$

Letting $\rho(\mathcal{E},\tau)$ be the probability density for finding the system with mechanical energy $\mathcal{E}$, *i.e.* $\mathbf{v} = \mathbf{P}_0\rho$, and using eq. (5) a Fokker-Planck equation for ρ is obtained;

$$\begin{aligned}\frac{\partial}{\partial\tau}\rho(\mathcal{E},\tau) &= -\frac{\partial}{\partial\mathcal{E}}[(\mathcal{W}(\mathcal{E}) - \gamma(\mathcal{E}) + \mathcal{O}(\epsilon^2))\rho(\mathcal{E},\tau)] \\ &- \epsilon^2\frac{\partial^2}{\partial\mathcal{E}^2}\left(\sum_{\lambda\neq 0}\frac{f_\lambda(\mathcal{E})g_\lambda(\mathcal{E})}{\lambda(\mathcal{E})}\rho(\mathcal{E},\tau)\right),\end{aligned}$$

where $f_\lambda(\mathcal{E}) \equiv \int_0^{2\pi} d\phi\mathbf{Q}_0^*\cdot\hat{\mathcal{O}}\mathbf{P}_\lambda(\mathcal{E},\phi)$ and $g_\lambda(\mathcal{E}) \equiv \int_0^{2\pi} d\phi\mathbf{Q}_\lambda^*\cdot\hat{\mathcal{O}}\mathbf{P}_0(\mathcal{E},\phi)$, with $\hat{\mathcal{O}} \equiv \left[2\eta\mathcal{E}\cos^2\phi - 2\hat{f}\sqrt{\mathcal{E}}\cos\phi\right]$. Since $(\mathcal{W}(\mathcal{E}) - \gamma(\mathcal{E}))$ is of order ϵ the small energy shift of order ϵ^2 can be ignored to a first approximation and an equivalent Ito stochastic differential equation for the vibrational energy $\mathcal{E}$ is arrived at

$$d\mathcal{E} = [\mathcal{W}(\mathcal{E}) - \gamma(\mathcal{E})]\,d\tau + \alpha(\mathcal{E})dW(\tau),$$

where $W(\tau)$ is the Wiener process and $\alpha(\mathcal{E}) \equiv \epsilon\sqrt{-2\sum_{\lambda\neq 0} f_\lambda(\mathcal{E})g_\lambda(\mathcal{E})}$.

Performing a small noise expansion [28] around $\mathcal{E}_0$, where $\mathcal{E}_0$ solves $(\mathcal{W}(\mathcal{E}_0) - \gamma(\mathcal{E}_0)) = 0$, an analytical expression for the PSD can be obtained

$$S_{II}(\omega) = 2\frac{[\alpha(\mathcal{E}_0)I'(\mathcal{E}_0)]^2}{(\gamma'(\mathcal{E}_0) - \mathcal{W}'(\mathcal{E}_0))^2 + \omega^2}. \tag{6}$$

Here the current I is given by $I(\mathcal{E}) = \frac{e\omega}{2\pi}\int_0^{2\pi} d\phi \mathbf{Q}_0^* \cdot \hat{\mathcal{J}}(\mathcal{E},\phi)\mathbf{P}_0(\mathcal{E},\phi)$. where $\left(\hat{\mathcal{J}}(\mathcal{E},\phi)\right)_{i,j} \equiv \delta_{i,j}\tilde{\Gamma}^{\mathrm{R}}_{n(i)\to n(i)-1}(\mathcal{E},\phi) - \tilde{\Gamma}^{\mathrm{R}}_{n(i)\to n(i)+1}(\mathcal{E},\phi)$ is the current operator.

Equation (6) is our central result. Two important conclusions can be drawn from this equation. First, below a break frequency given by $\omega_c = (\gamma'(\mathcal{E}_0) - \mathcal{W}'(\mathcal{E}_0))$ the noise will rise due to fluctuations in oscillation amplitude. This agrees with the PSD in fig. 2. Second, approaching the transition point (from above) $(\gamma'(\mathcal{E}_0) - \mathcal{W}'(\mathcal{E}_0)) \to 0$ (see ref. [10]) which implies that the low frequency noise may display a divergent behavior at the point of transition from shuttle to stationary regime.

To investigate this eqs. (1-2) were simulated for a sequence of voltages for one typical system and the resulting $I - V$ curve as well as the Fano factor are shown in fig. 3. The parameter values used are shown in table 1. They correspond to a nanometer sized Au grain commonly used in experiments with self-assembled Coulomb blockade double junctions.

Although, as explained in [13], the non-parabolic confining potential smoothens any step-structure in the current-voltage characteristics, the transition between static- and shuttle-operation is clearly visible in the noise spectrum. Below the threshold voltage the Fano factor is of the order 1/2 whereas in the shuttle regime, it is higher. In accordance with eq. 6, approaching the threshold from above (higher to lower voltages) the PSD shows divergent behavior.

5 Conclusions

Using adiabatic elimination of fast variables and numerical integration of eqs. (1-2) the PSD of the classical single electron shuttle has been studied in the case of weak electromechanical coupling. We have focussed on the low frequency part of the spectrum, which is the part most susceptible to direct measurements, and found that the shuttle regime can be distinguished from the stationary regime by the noise level at low frequencies.

In particular, the shuttle regime is associated with a rise in the low frequency PSD, as compared to a stationary Coulomb blockade double junction, resulting in an increased Fano factor. This increase is due to slow variations in the current arising from variations in oscillation amplitude. Approaching the point of the transition from above (lowering the bias voltage when in the shuttle regime) the noise level shows a (quasi) divergent behavior upon closing in on the transition. Hence, even though a measurement of the average current alone may not reveal whether the system is in the shuttle regime or not, the accompanying noise signature can provide this information.

6 acknowledgments

The authors are grateful for stimulating discussions with R. I. Shekhter and L. Y. Gorelik. This work has received financial support (A.I.) through The Swedish Foundation for International Cooperation in Research and Higher Education (STINT), and (T.N.) the Swedish Research Council (VR).

References

[1] BLANTER YA. M. and BUTTIKER M., *Phys. Rep.*, **336**, (2000) 1.

[2] HANKE U., GALPERIN Y. M., CHAO K. A. and ZOU N.,*Phys. Rev. B*, **48**, (1993) 48.

[3] ROUKES M, *Phys. World* **February**, (2001) 25; CRAIGHEAD H. G., *Science* **290**, (2000) 1532.

[4] GORELIK L.Y., *et al.*,*Phys. Rev. Lett.* **80**, (1998) 4526.

[5] ERBE A. *et al.*,*Appl. Phys. Lett.*, **73**, (1998) 3751: ERBE A, WEISS C., ZWERGER W. and BLICK R.H., *Phys. Rev. Lett.* **87**, (2001) 096106.

[6] SCHEIBLE D.V., ERBE A., and BLICK R.H.,*New J. Phys.*, **4**, (2002) 86.1.

[7] PARK H. *et al.*, *Nature* (London) **407**, (2000) 57.

[8] NAGANO K, OKUDA A., and MAJIMA Y., *Appl. Phys. Lett.* **81**, (2002) 544.

[9] TUOMINEN M.T., KROTKOV R.V., and BREUER M.L., *Phys. Rev. Lett.*, **83**, (1999) 3025.

[10] ISACSSON A. *et al.*,*Physica B*, **255**, (1998) 150.

[11] NISHIGUCHI N., *Phys. Rev. B*, **65**, (2001) 035403.

[12] NORD T., *et al.*, *Phys. Rev. B*, **65**, (2002) 165312.

[13] NORD T., ISACSSON A.,*Phys. Rev. B*, **69**, (2004) 035309.

[14] WEISS C., ZWERGER W.,*Europhys. Lett.* **47**, (1999) 97.

[15] NISHIGUCHI N., *Phys. Rev. Lett.*, **89**, (2002) 66802.

[16] BOESE D., H. SCHOELLER H., *Europhys. Lett.*, **54**, (2001) 668.

[17] FEDORETS D. *et al.*, *Europhys. Lett.* **58**, (2002) 99.

[18] ARMOUR A.D., and MACKINNON A.,*Phys. Rev. B*, **66**, (2002) 035333.

[19] FEDORETS D, *Phys. Rev. B*, **68**, (2003) 033106.

[20] NOVOTNÝ T., DONARINI A., and JAUHO A.-P., *Phys. Rev. Lett.*, **90**, (2003) 256801.

[21] MCCARTHY K.D., PROKOF'EV N., and TUOMINEN M.T.,*Phys. Rev. B*, **67**, (2003) 245415.

[22] BRAIG S. and FLENSBERG K. *Phys. Rev. B.*, **68**, (2003) 205324.

[23] GORELIK L.Y. *et al.*, *Nature* (London) **411**, (2001) 454; ISACSSON A. *et al.*, *Phys. Rev. Lett.* **89**, (2002) 277002.

[24] SHEKHTER R.I. *et al.*, *J. Phys.: Condens. Matter*, **15**, (2003) 441.

[25] KULIK I.O. and SHEKHTER R.I., *Sov. Phys. JETP*, **41**, (1975) 308.

[26] ISRAELACHVILI J.N., *Intermolecular and Surface Forces*, (Academic Press London) 1985.

[27] DE JONG M.J.M. and BEENAKKER C.W.J., in *Mesoscopic electron transport*, edited by L.L. SOHN it et al., (Kluwer, Netherlands).

[28] GARDINER C.W., *Handbook of Stochastic Methods*, 2nd ed. (Springer-Verlag Berlin Heidelberg) 1997.

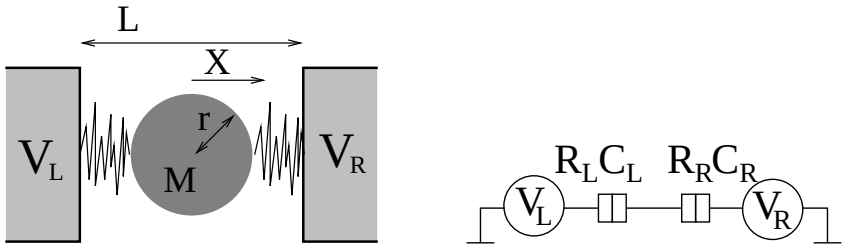

(a) (b)

Figure 1: Single electron shuttle. (a) A metallic grain of mass M and radius r placed between two leads separated by a distance L. The displacement of the grain from the center of the system is labelled X. The grain is connected to the leads via insulating elastic materials. The leads are biased to the potentials V_L and V_R. (b) Equivalent circuit of the system. The tunneling resistances and capacitances of the left and right junctions are R_L, R_R, C_L, and C_R.

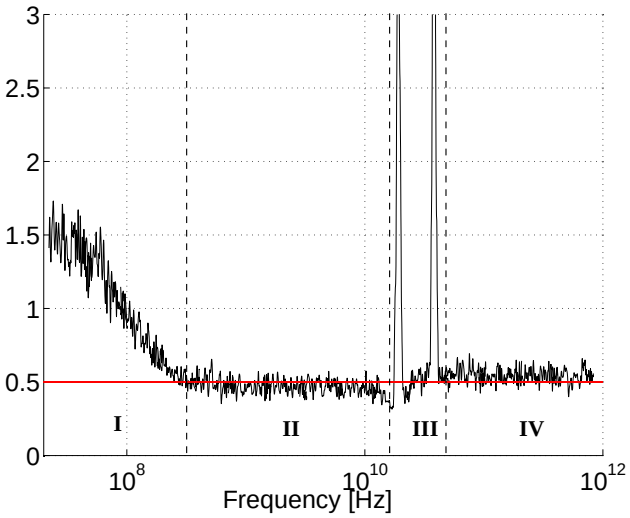

Figure 2: Power spectrum $S_{II}(\omega)$ for large amplitude shuttling. For frequencies above the vibrational frequency the Fano factor is close to 1/2 as for a static Coulomb blockade junction. The peaks are located at the frequency of vibration and at the first harmonic. For frequencies below the vibrational frequency, the in time correlation due to the periodic grain motion leads to a slight suppression of the noise level. At still lower frequencies the the noise is increased due to slow fluctuations in oscillation amplitude.

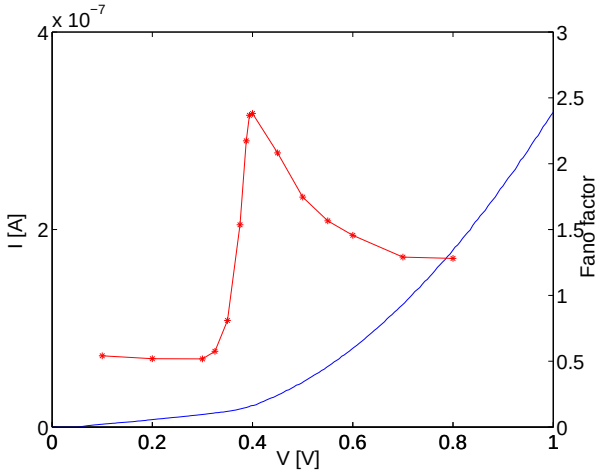

Figure 3: Current voltage characteristics plotted together with $S_{II}(\omega \to 0)$. The current is the solid line with the scale on the left ordinate while the Fano factor is shown for a discrete set of points with the scale on the right ordinate (Lines connecting the points are a guide to the eye). Below the critical voltage where there is no sustained grain motion the Fano factor is that of a Coulomb blockade double junction. Above the critical voltage the grain is oscillating and the Fano factor is increased and shows a divergent behavior at the critical voltage in accordance with eq. (6).

Table 1: Numerical values of parameters used to obtain data of fig. 3.

Quantity	Value	Units	Quantity	Value	Units	Quantity	Value	Units
L	5	nm	k	1	N/m	λ	0.1	nm
r	1	nm	X_L,X_R	1	nm	R_0^L,R_0^R	10	$M\Omega$
M	10^{-23}	kg	H_a	$4 \cdot 10^{-19}$	Nm	C_0^L,C_0^R,C_0	1	aF
γ	10^{-13}	kg/s	H_r	10^{-72}	Nm^7	A_L,A_R	2.5	nm